Electronic Supplementary Information for:

Engineering high-performance and air-stable PBTZT-stat-BDTT-8:$PC_{61}BM$/$PC_{71}BM$ organic solar cells

Il Jeon,[a] Ryohei Sakai,[b] Seungju Seo,[a] Graham E. Morse,[c] Hiroshi Ueno,[d] Takafumi Nakagawa,[a] Yang Qian,[a] Shigeo Maruyama,[a,e] Yutaka Matsuo[a,f]*

a: Department of Mechanical Engineering, School of Engineering, The University of Tokyo, 7-3-1 Hongo, Bunkyo-ku, Tokyo 113-8656, Japan

b: Fujipream Corporation, 38-1 Shikisai, Hyogo 671-2216, Himeji, Japan

c: Merck Chemicals Ltd., Chilworth Technical Centre, University Parkway, SO16 7QD Southampton, UK

d: School of Chemistry, Northeast Normal University, Changchun, Jilin 130024, China

e: National Institute of Advanced Industrial Science and Technology (AIST), 1-2-1 Namiki, Tsukuba, Ibaraki 305-8564, Japan

f: Hefei National Laboratory for Physical Sciences at the Microscale, University of Science and Technology of China, Hefei, Anhui 230026, China

E-mail: (Y.M) matsuo@photon.t.u-tokyo.ac.jp

1. Differential Pulse Voltammetry

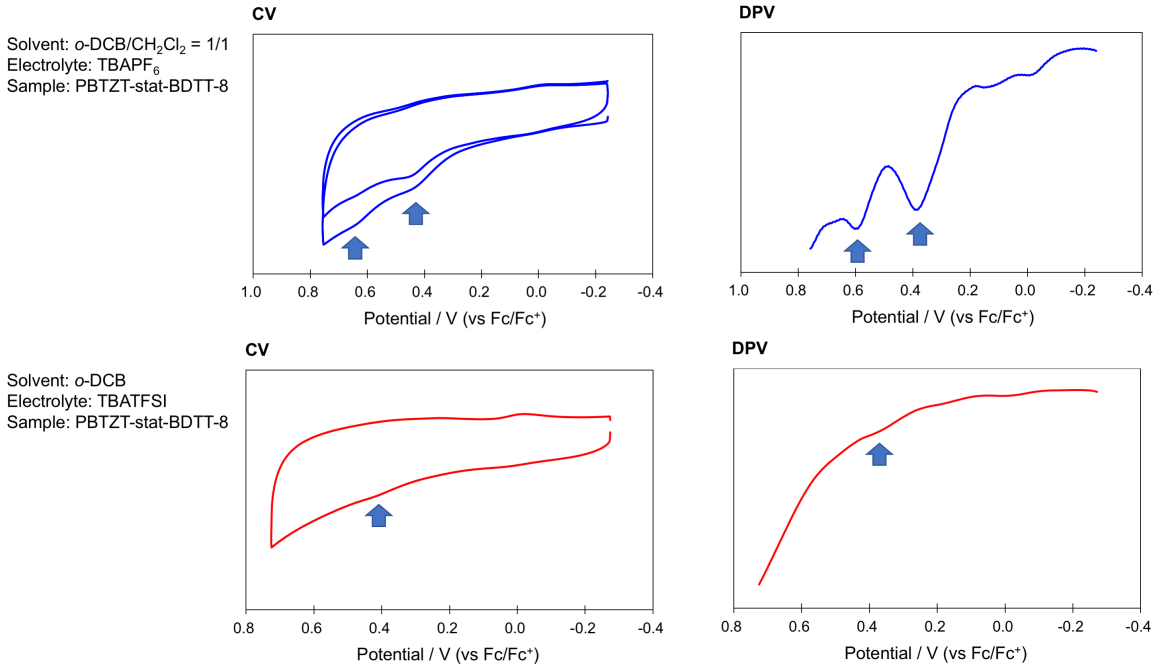

Fig. S1 CV (left) and DPV (right) of PBTZT-stat-BDTT-8 in different solvents and electrolytes.

2. Device Optimisation

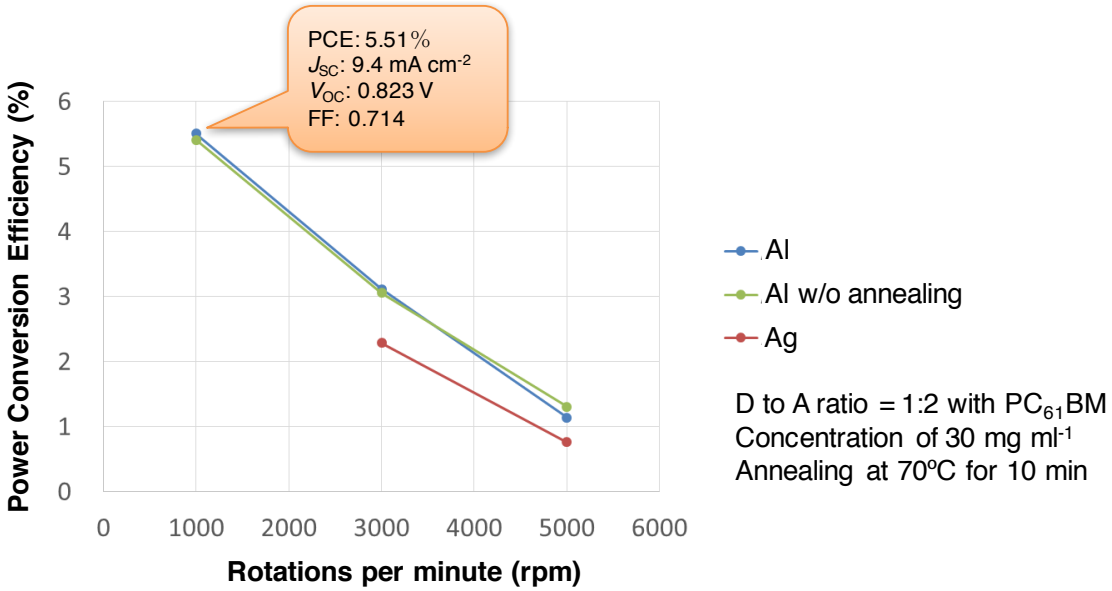

- Al as the electrode performs better than Ag
- Thicker the active layer, the better the performance

Fig. S2 Cathode selection experiment.

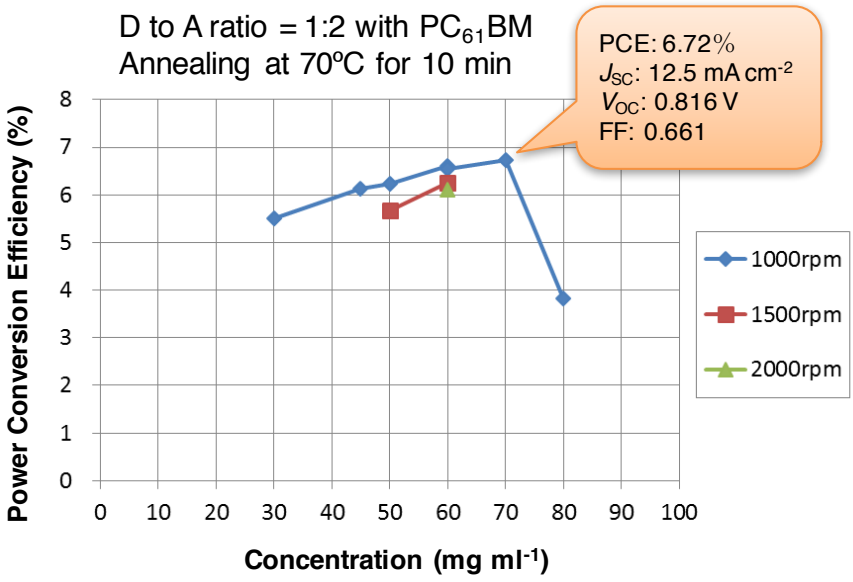

- 1000 rpm with 70 mg ml^{-1} concentration was optimum
- 80 mg ml^{-1} seemed to be blocked by the filter

Fig. S3 Film thickness optimisation.

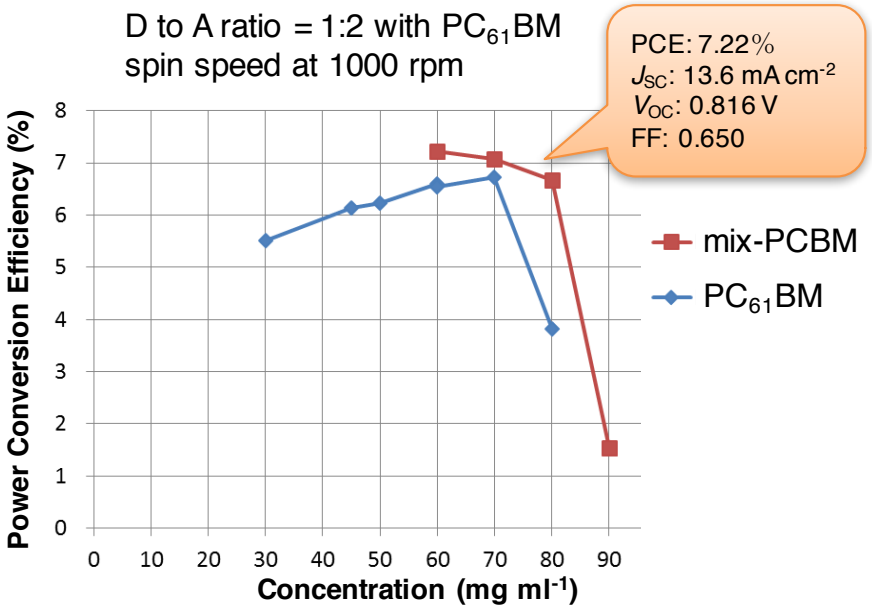

- mix-PCBM performs better than $PC_{61}BM$
- optimum concentration for mix-PCBM is 60 mg ml^{-1}

Fig. S4 Optimisation using $PC_{61}BM$ and mix-PCBM.

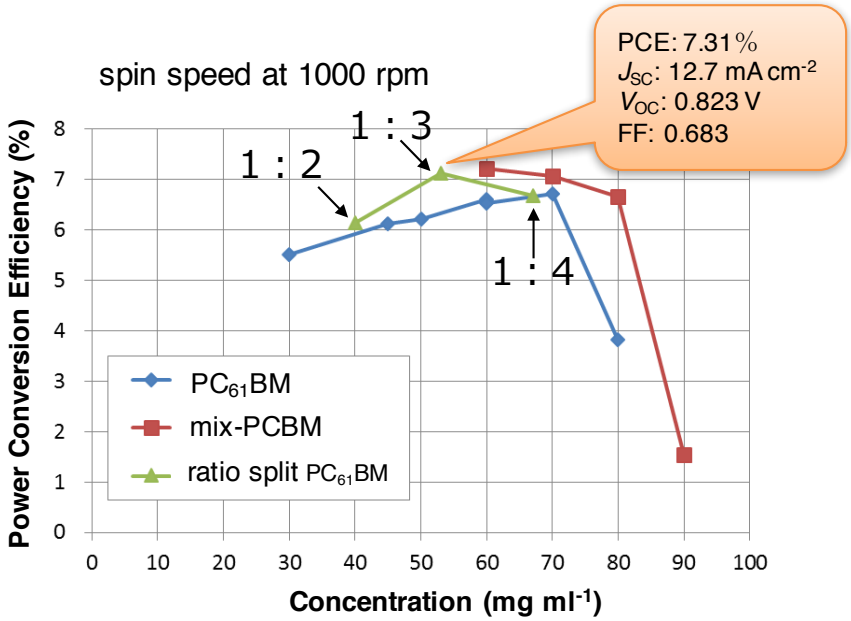

- 1:3 D to A ratio performed the best

Fig. S5 Donor to acceptor ratio optimisation.

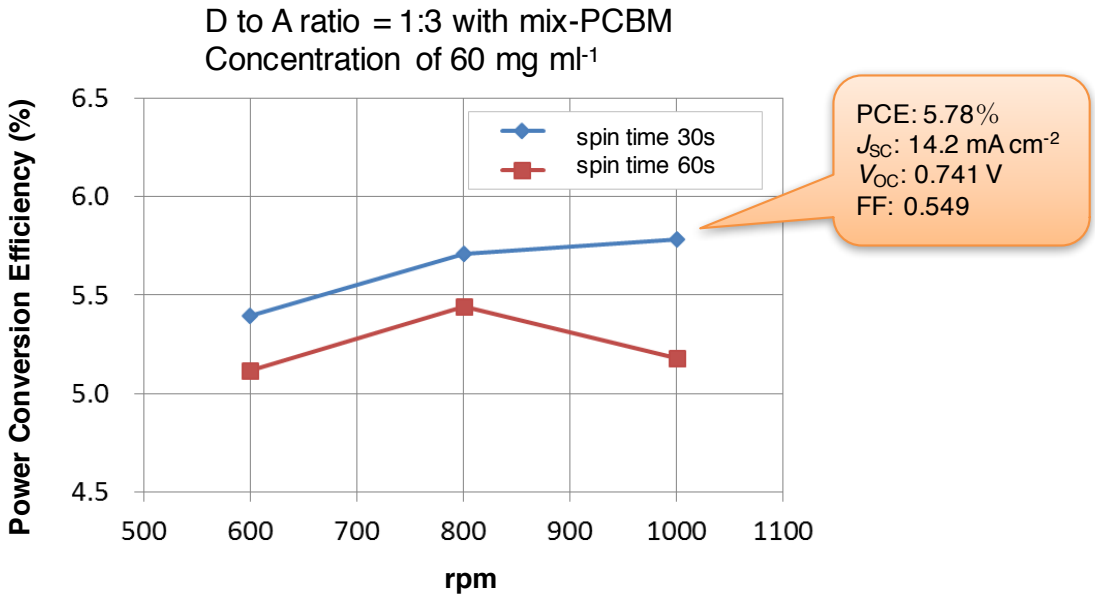

Fig. S6 Spin-coating time split test.

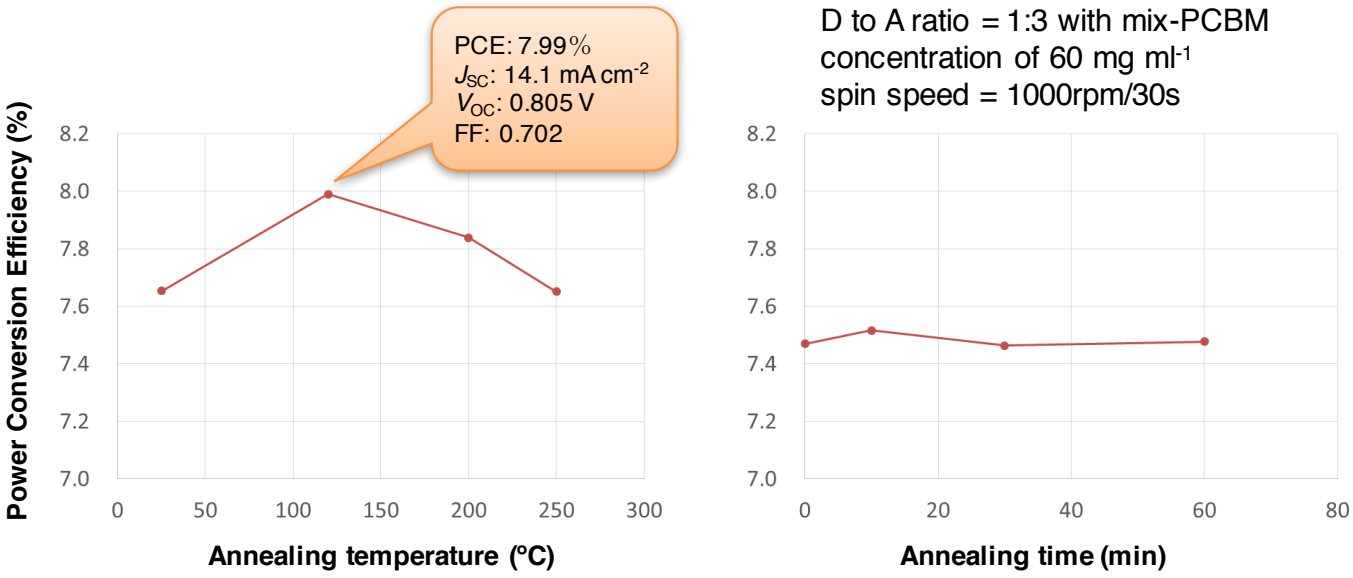

Fig. S7 Annealing temperature and time optimisation.

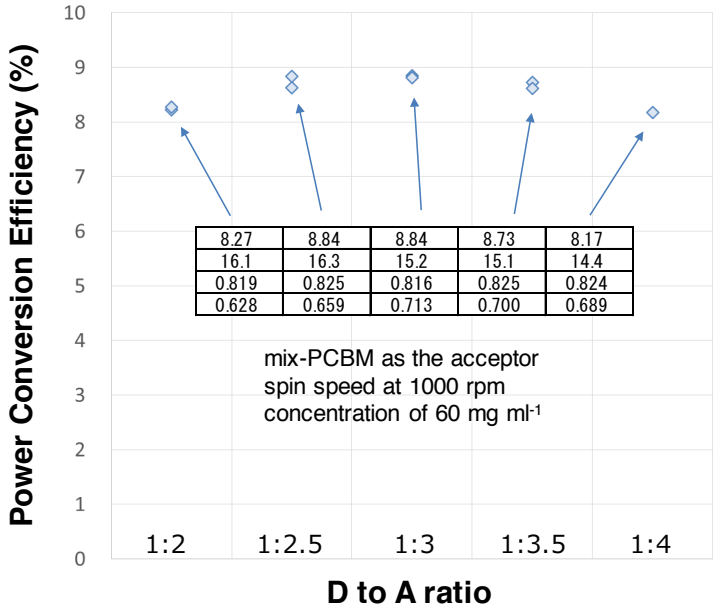

Fig. S8 Donor to acceptor ratio optimisation for the inverted architecture with mix-PCBM.

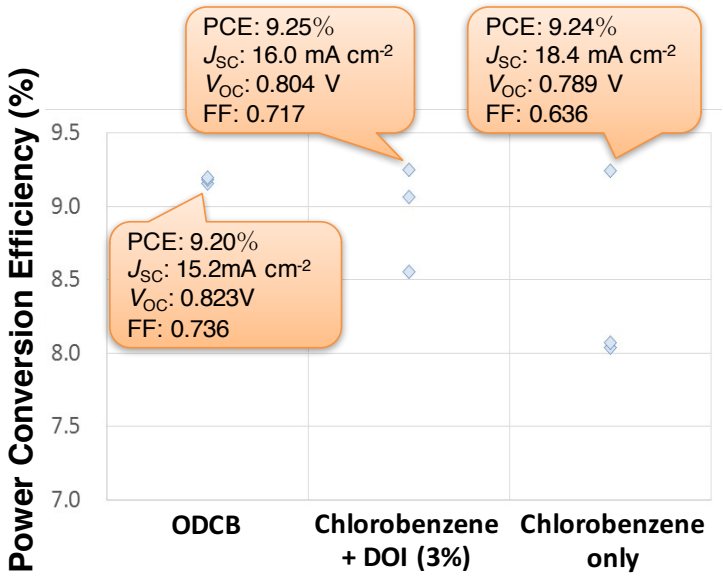

Fig. S9 PCEs of PBTZT-stat-BDTT-8-based solar cells with different types of solvents.

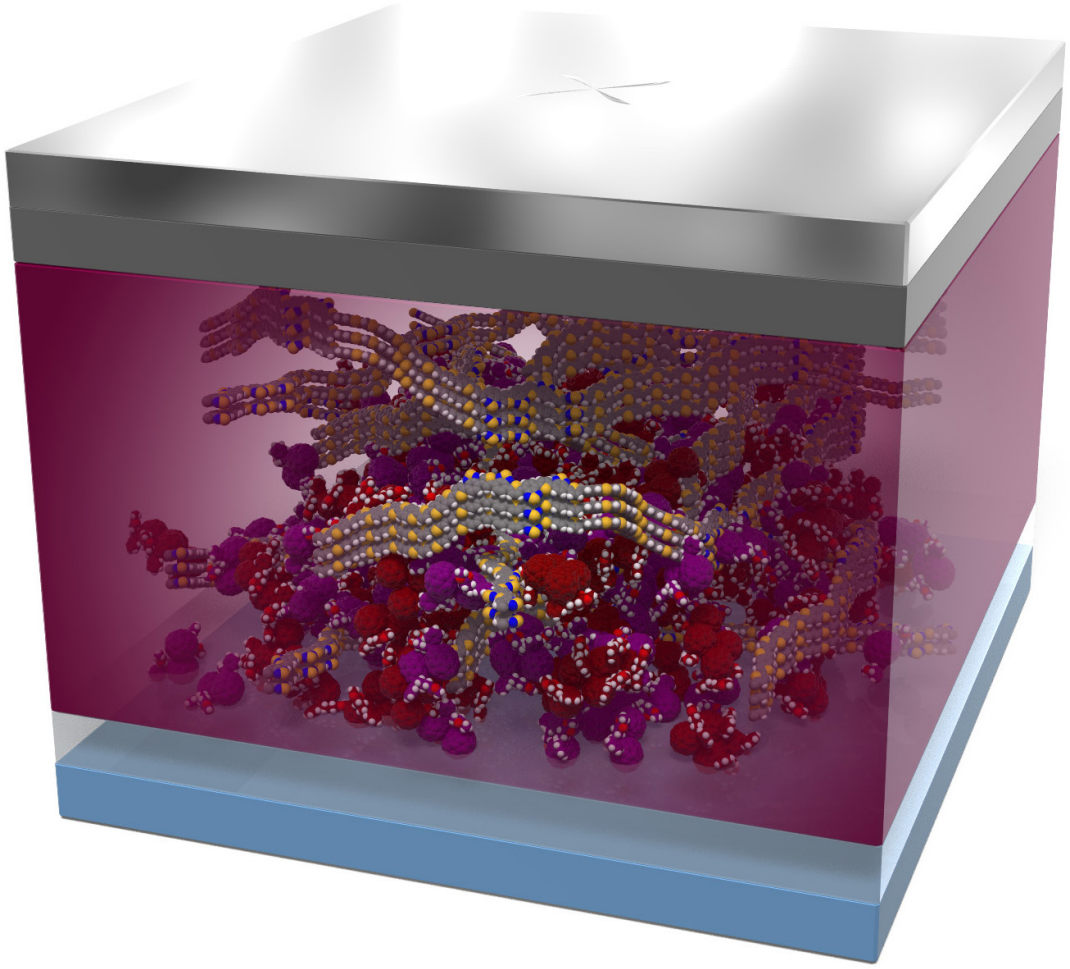

Fig. S10 Schematic drawing for vertical separation in the blend

3. Heterojunction Blend Stability

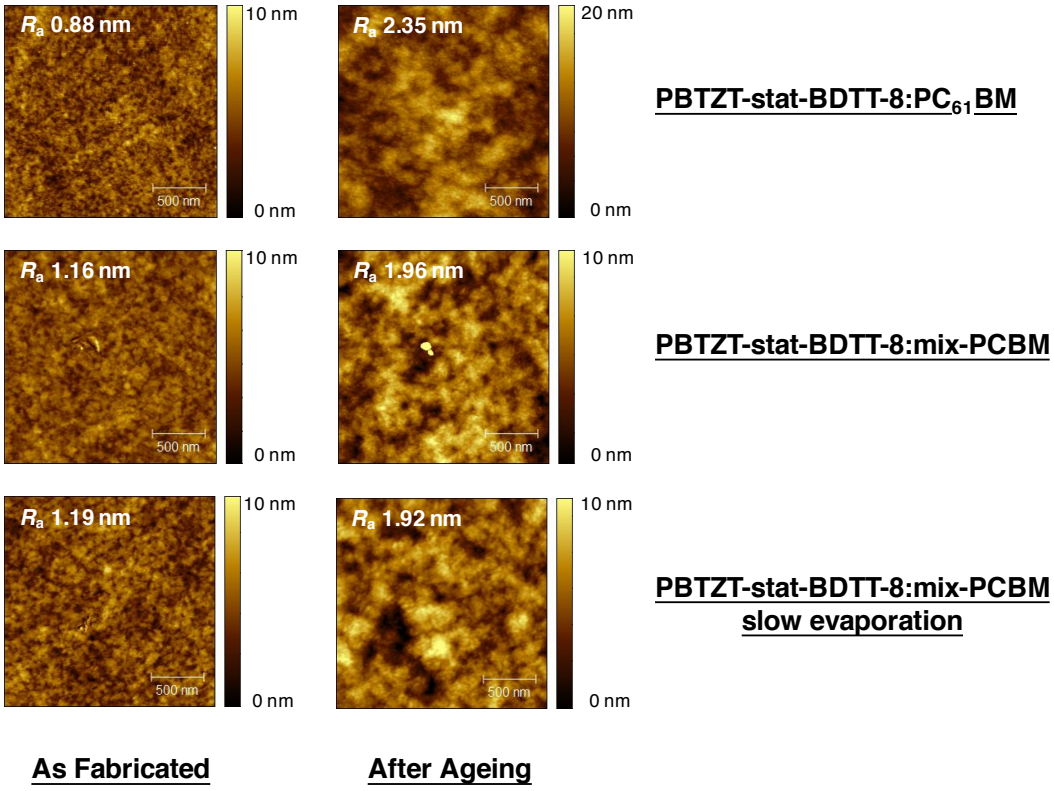

Fig. S11 AFM images and roughness before and after thermally ageing at 200 °C for 2 hours in air (60% relative humidity).

Table S1. SCLC hole and electron mobility measurements of PBTZT-stat-BDTT-8 mixed with different PCBM.

Type	Active Layer	Mobility, μ ($cm^2 V^{-1} s^{-1}$)
Hole mobility	PBTZT-stat-BDTT-8:$PC_{71}BM$	4.3×10^{-5}
	PBTZT-stat-BDTT-8:$PC_{61}BM$	8.0×10^{-5}
	PBTZT-stat-BDTT-8:mix-PCBM	1.0×10^{-4}
Electron mobility	PBTZT-stat-BDTT-8:$PC_{71}BM$	1.0×10^{-3}
	PBTZT-stat-BDTT-8:$PC_{61}BM$	1.2×10^{-3}
	PBTZT-stat-BDTT-8:mix-PCBM	4.1×10^{-4}
Hole mobility after ageing	PBTZT-stat-BDTT-8:$PC_{71}BM$	4.7×10^{-4}
	PBTZT-stat-BDTT-8:$PC_{61}BM$	1.9×10^{-5}
	PBTZT-stat-BDTT-8:mix-PCBM	3.2×10^{-4}

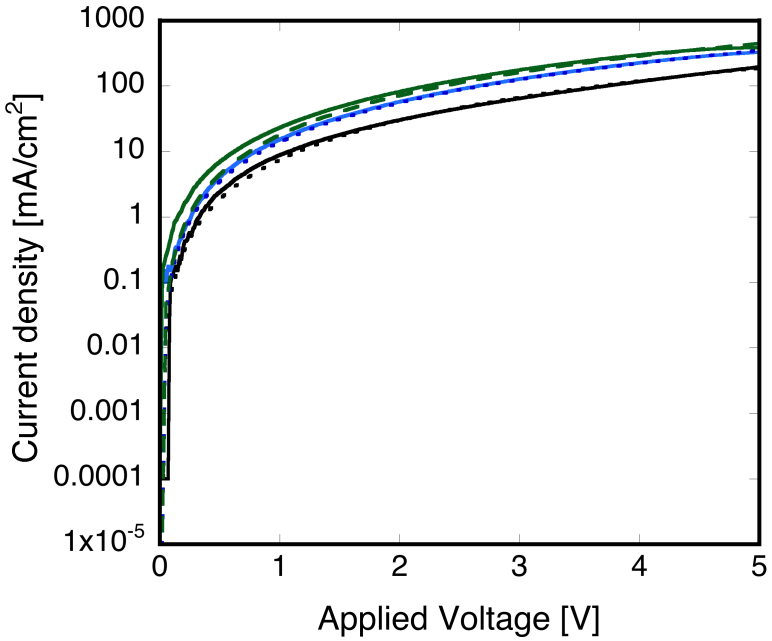

Fig. S12 Fitting chart of the hole-only devices (The black line is for the $PC_{71}BM$-mixed blend, the blue line is for the $PC_{61}BM$-mixed blend, and the green line is for the mix-PCBM-blend. The dotted lines are the fitting curves)

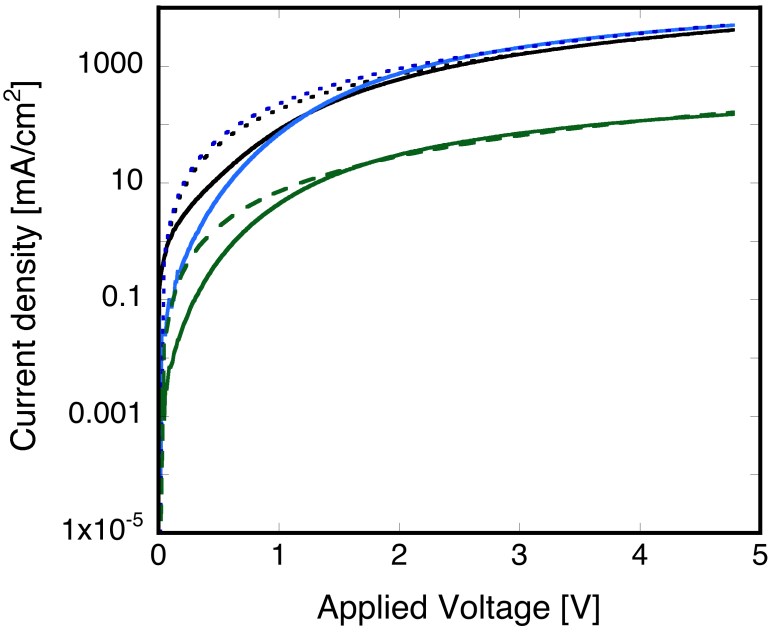

Fig. S13 Fitting chart of the electron-only devices (The black line is for the $PC_{71}BM$-mixed blend, the blue line is for the $PC_{61}BM$-mixed blend, and the green line is for the mix-PCBM-blend. The dotted lines are the fitting curves)

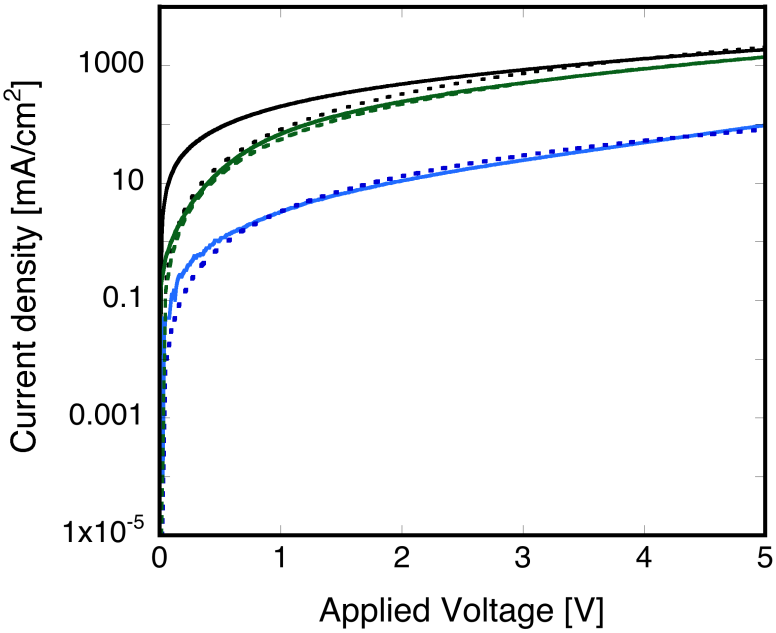

Fig. S14 Fitting chart of the hole-only devices after ageing (The black line is for the $PC_{71}BM$-mixed blend, the blue line is for the $PC_{61}BM$-mixed blend, and the green line is for the mix-PCBM-blend. The dotted lines are the fitting curves)

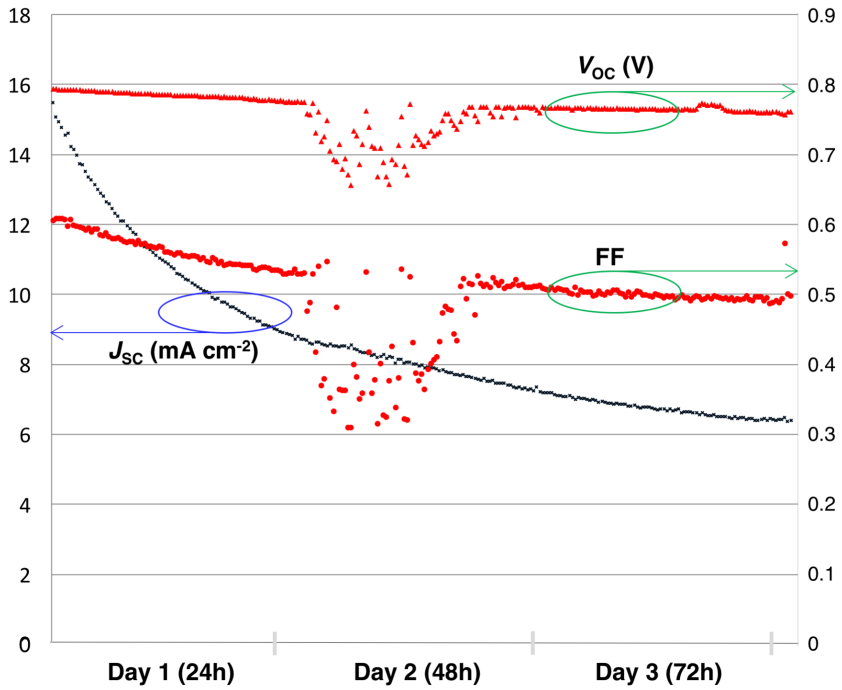

Fig. S15 Stability of unencapsulated PBTZT-stat-BDTT-8:mix-PCBM OSCs under constant illumination of 1 sun in humid air (40 °C, 50% relative humidity) for J_{SC} (black dot), V_{OC} (red triangle), and FF (red circle).